

ANALYSIS OF FRACTURE NETWORKS OF THE BLACK VOLTA CATCHMENT IN CÔTE D'IVOIRE

ABSTRACT

The good knowledge of fracturing leads to a better exploitation of the groundwater of the areas in crystalline basement. This study interests the catchment of Black Volta area in northeastern Côte d'Ivoire, its aims to characterize the fracture networks of the catchment of black Volta. Various methods are used notably mapping using satellite image processing, statistical and geostatistical analysis.

The results showed that fracturing of Black Volta area is dense and homogeneous. Statistical analysis of geometric parameter of the fracturing such fracture lengths and spacing are distributed **respectively** according to the power law and gamma law. The deployment of the fracturing in this area is organized and the experimental variogram is characterized by two nested elementary structures. The practical ranges of these two elementary variograms are respectively equal to $a_1 = 34, 5$ km and $a_2 = 60$ km. Results indicate that the fracturing of black Volta area reached a stage of advanced development and is complex. Fracturing of Black Volta area is now well known and the groundwater modeling can be undertaking.

Keywords: *Black Volta, Côte d'Ivoire, satellite image, fracture analysis, statistical, geostatistical.*

INTRODUCTION

Groundwater meet in crystalline and metamorphic rocks preferentially in the aquifers fissured. In this media three aquifers were identified: weathering **materiel**, fissured zone and the faults aquifers (Wyns et al., 1999). **These aquifers had the advantage to be at safe of seasonal fluctuations and possible accidental pollution** (Lasm, 2000; Jourda, 2005).

However these systems present a very complex configuration (**Biémi, 1992; Savané, 1997**). The fractures have geometrical and hydrodynamic properties extremely variable. These last decades,

the fractured mediums were abundantly studied. In Côte d'Ivoire several studies (**Kouamé, 1999; Lasm, 2000; Jourda, 2005, Lasm et al., 2008; Youan Ta, 2008; Youan Ta et al., 2008; Yao, 2009**) were carried out and contributed to the knowledge of this medium which covers 97.5% of national territory.

In the basin of Black Volta in eastern Côte d'Ivoire very few studies exist (Goula and Egnankou, 2011) **and this basin is badly know in hydrogeology point of view**. Complete studies were carried out by **Youan Ta (2008) and Jofack-Sokeng (2013)** in Bondoukou area. The present

study interest the part of Black Volta basin were study are sparse. It aims to analyze the networks of fractures from a statistical point of view for a better knowledge of their water resources.

Geographical, geological and hydrogeological context of study area

The study area is the part of transborder basin of Black Volta in Côte d'Ivoire. It covers a surface of 12950 km². It is located between the latitudes 7°78 and 9°94 N and longitudes 2°49 and 3°35 W and is situated in the extreme North-Eastern Côte d'Ivoire.

In a geological point of view, this area is situated on the Paleozoic crystalline basement.

It was affected by three orogenesis (Leonean, Liberian and eburnean) which contributed to the structuring of the two principal geological domains of Côte d'Ivoire: the archaean and paleo-proterozoic domains respectively in the west and east parts and separated by the major fault of Sassandra. In petrographic point of view, this area is constituted mainly of schists, gneisses and granitoid (figure 1). On the level hydrogeologic, three aquifers were distinguished weathering aquifer, the fissured aquifer and faults aquifer

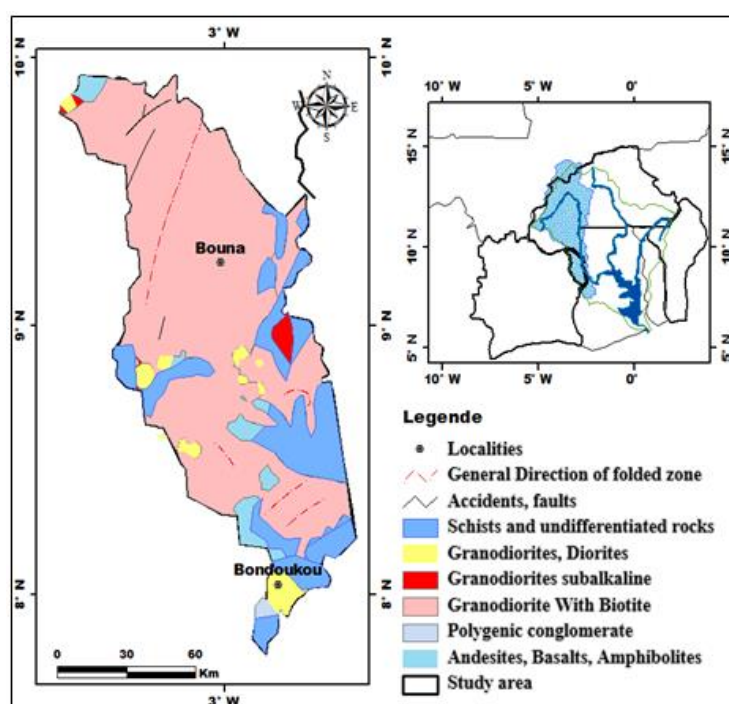


Figure 1: Geological map of study area

2. METHODOLOGY

2.1. Methodology of processing data for the structural cartography

Pretreatment of satellite images

Various techniques were carried out on the rough satellite images before the treatment itself with an aim of facilitating their interpretation. A mosaic was carried out in the extreme starting from four scenes of sensor OLI of Landsat 8.

The radiometric and atmospheric correction was applied to increase the legibility of data by correcting certain

variations of the distribution of those caused by the noises atmospheric and radiometric. In the same way a harmonization of the histograms by the method of equalization of histogram contributed to improve apparent contrast on the mosaic of the scenes. The essence of these operations was carried out on these last including/understanding seven bands selected among the nine bands collected by OLI (OLI2, OLI3, OLI4, OLI5, OLI6, OLI7 and OLI8 resampled to 30 m of resolution).

2.2. Digital processing of the satellite images

The methods applied for the image processing at the time of this study are three. One notes the analysis in principal components (ACP), the ratios bands and the techniques of filtering per drop window. The principal analysis in components (ACP), is a mathematical transformation based on the analysis of the covariance of the image or the matrix of correlation of several sets of data. It generates new component images which are in linear combination with the original images. This method was applied to the image resulting from the procedure of pretreatment. The ACPS made it possible to raise the quality of the multispectral images by eliminating the redundancy from the data contained in the various channels.

Two spectral zones were identified: the domain of visible (OLI2, OLI3 and OLI4) and the domain of the average infrared (OLI6 and OLI7) to which one can join the panchromatic band (OLI8).

Thus the ACP234 and ACP678 were carried out.

Certain structural information's contained in the image could be raised thanks to bands ratios which aim is to be reduced the sum of information or the description of particular topics on the images. The ratios bands carried out are: ratios OLI5/OLI7 (attenuation of shadow effect; OLI4 – OLI3/OLI4 + OLI3 (clearness index IC, for the description of the naked ground); OLI5 - OLI4/OLI5 + OLI4 (vegetation index NDVI); OLI7 – OLI8/OLI7 + OLI8, (enhancement of the regional lineament); OLI7/OLI5 (enhancement of the lineament from hydrographic network).

The technique of filtering per drop window was applied to generated news channels the to accentuate discontinuities images by using the gradients filters (Yésou, 1993) and directional of Sobel 7×7 calculated by assignment of higher weights on the level of convolution matrix. The Matrix presented below (table 1) accentuate the images discontinuities in the perpendicular directions to the convolution matrix.

Table 1. Directional filters of Sobel of size 7×7: a) NS; b) E-W; c) NE-SW and d) NW-SE

a) Filter of Sobel of NS direction						
1	2	3	4	3	2	1
2	3	4	5	4	3	2
3	4	5	6	5	4	3
0	0	0	0	0	0	0
-3	-4	-5	-6	-5	-4	-3
-2	-3	-4	-5	-4	-3	-2
-1	-2	-3	-4	-3	-2	-1

b) Filter of Sobel of E-W direction						
1	2	3	0	-3	-2	-1
2	3	4	0	-4	-3	-2
3	4	5	0	-5	-4	-3
4	5	6	0	-6	-5	-4
3	4	5	0	-5	-4	-3
2	3	4	0	-4	-3	-2
1	2	3	0	-3	-2	-1

d) Filter of Sobel of NW-SE direction						
4	3	3	2	2	1	0
3	5	4	4	3	0	-1
3	4	6	5	0	-3	-2
2	4	5	0	-5	-4	-2
2	3	0	-5	-6	-4	-3
1	0	-3	-4	-4	-5	-3
0	-1	-2	-2	-3	-3	-4

c) Filter of Sobel of NE-SW direction						
0	1	2	2	3	3	4
-1	0	3	4	4	5	3
-2	-3	0	5	6	4	3
-2	-4	-5	0	5	4	2
-3	-4	-6	-5	0	3	2
-3	-5	-4	-4	-3	0	1
-4	-3	-3	-2	-2	-1	0

Lineaments mapping was done manually by using the visual analysis of the enhanced images and/or filtered (first component of ACPs, indices and ratio bands).

The main part of the lineaments was indexed on these enhanced images using the filters of Yésou and Sobel (figure 2).

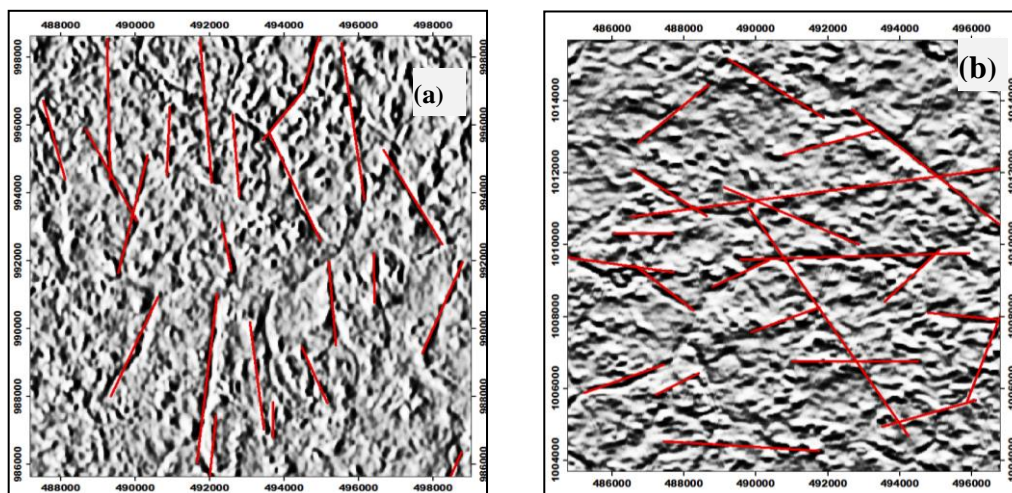


Figure 2: identification of the lineaments on filtered images (a) filters of Sobel E-NS enhanced the lineaments NS on CP1₂₃₄; (b); filter of Yésou enhanced the lineaments.

2.3. Statistical and geostatistical analysis of fractures network

Fractures network was analyzed according the statistical and geostatistical point of view. The statistical analysis consisted to study the distribution law of fractures length and spacing. Geostatistical analysis consisted to study the experimental variogram.

In this study the exponential model was used and defined by equation 1:

$$\gamma(h) = C_0 + C \times (1 - \exp(\frac{-3h}{a})) \quad (1)$$

With a : practical range; h : the distance between sampling point; $C+C_0$: the sill and C_0 : nugget effect.

ENVI 5.1 (Environment for Visualizing Image) was used for the image processings and lineaments mapping. Program RAFESP was used to calculate fractures spacing. Statistical and geostatistical analyses are carried out using software Statistica 7.1 and Variowin (Pannatier, 1996) respectively.

2.4. Control and validation

The control and validation of the extracted lineaments are essential to judge relevance of the method used. Control phase consisted to eliminate the artificial or manmade lineament (railroad, roads, tracks, telephone line, limiting lines of fields, park, etc.) beforehand mapped. Lineaments mapped were confronted with the fracturing map, the hydrographic network and productive drillings with large flows of the area in order to confirm their structural origin. The identified fractures were analyzed using frequential analysis and compared to fracture directions from geological map of the study area and earlier former work (Youan Ta et al, 2008; Jofack-Sokeng, 2014). The fracturing map obtained constitute a useful support for a better knowledge of fissured aquifers.

3. RESULTS AND DISCUSSION

3.1. RESULTS

➤ Satellite image processing

Atmospheric and radiometric corrections applied to the images led to new images which appear clearer, and the linearities are more perceptible on these last compared to the raw image (figure 3). This processing increases the legibility of data by correcting the distribution variations of data caused by the atmospheric and radiometric noises.

Figure 4 presents respectively the first (CP1₂₃₄) and third (CP3₂₃₄) component obtained by the application of the ACPs. Results of the first component of ACPs show that the process enhance the quality of multispectral images. Results of bands ratios carried out are presented at figure 5. Figure 5 illustrates well the aptitude of arithmetic ratios to highlight the information searched on the images. Vegetation index shows the vegetable cover brings the geomorphological information on the study area and the clearness index reduces the granular aspect of the raw images and highlights the naked ground. These images revealed each of interesting discontinuities.

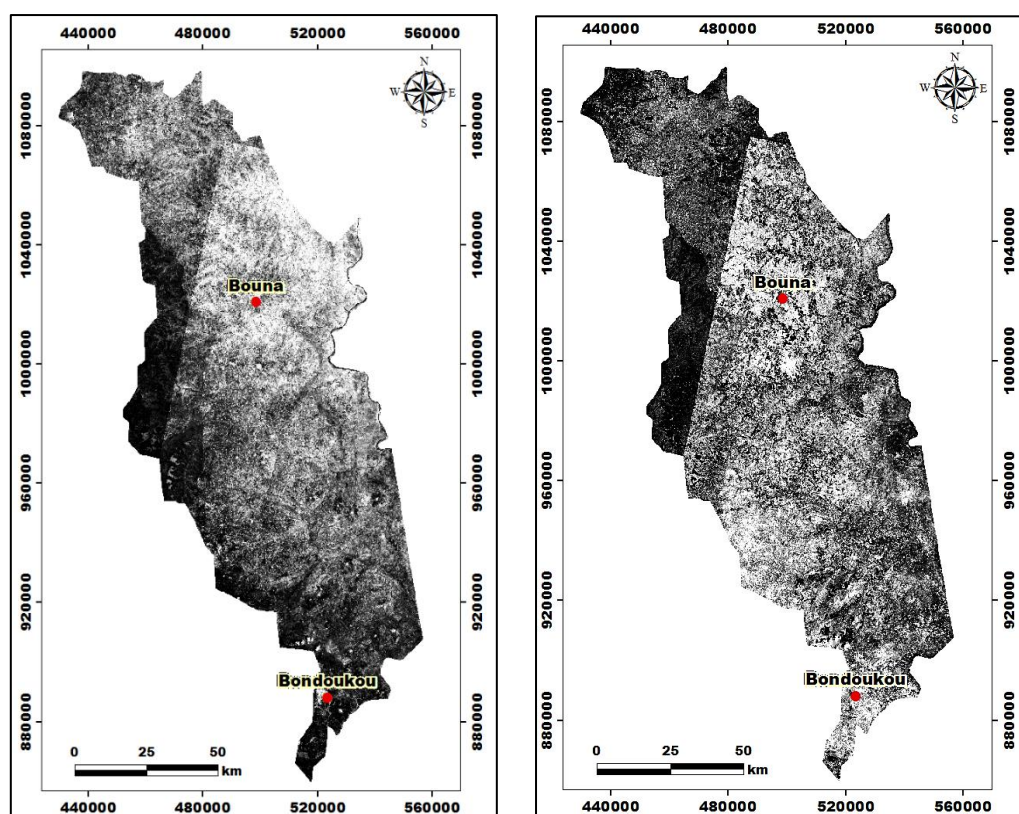


Figure 3. Result of the atmospheric correction on raw image of the study area: raw image OLI4 (A); image OLI4 corrected (B).

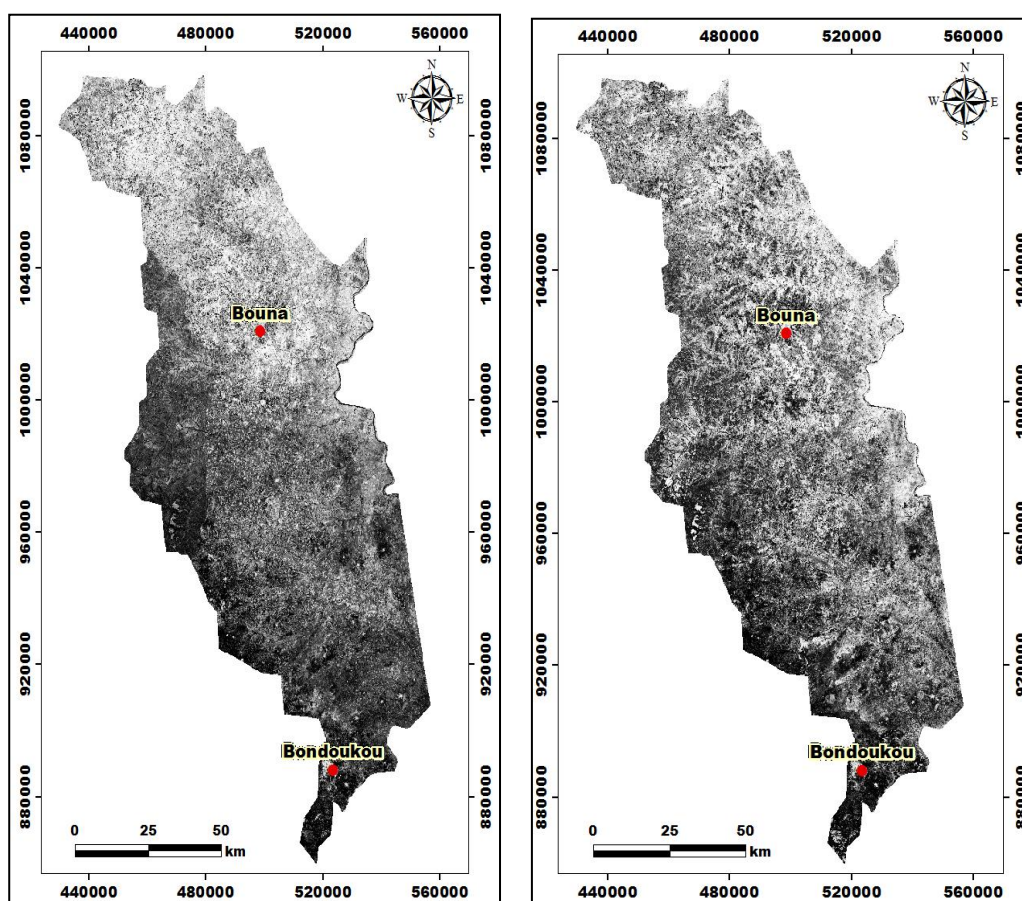


Figure 4. News channels resulting from ACP: (CP1₂₃₄) (a); (CP3₂₃₄) (b)

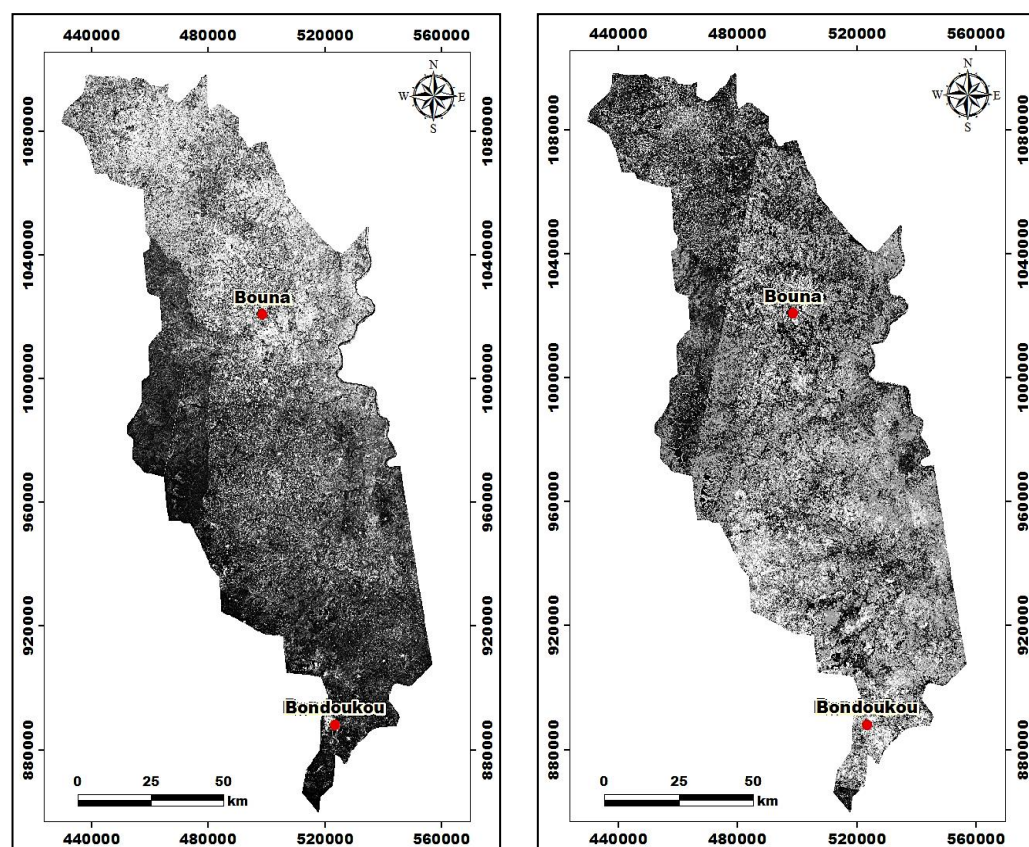


Figure 5. Results of ratios bands: vegetation index, NDVI (A); the clearness index IC (B)

The various techniques used for the satellite image processing generated new images more improved which were used as support for the structural mapping.

The resulting map presents numerous lineament of variable sizes that extend over several orders of magnitude revealing the strong heterogeneity of the area (figure 6).

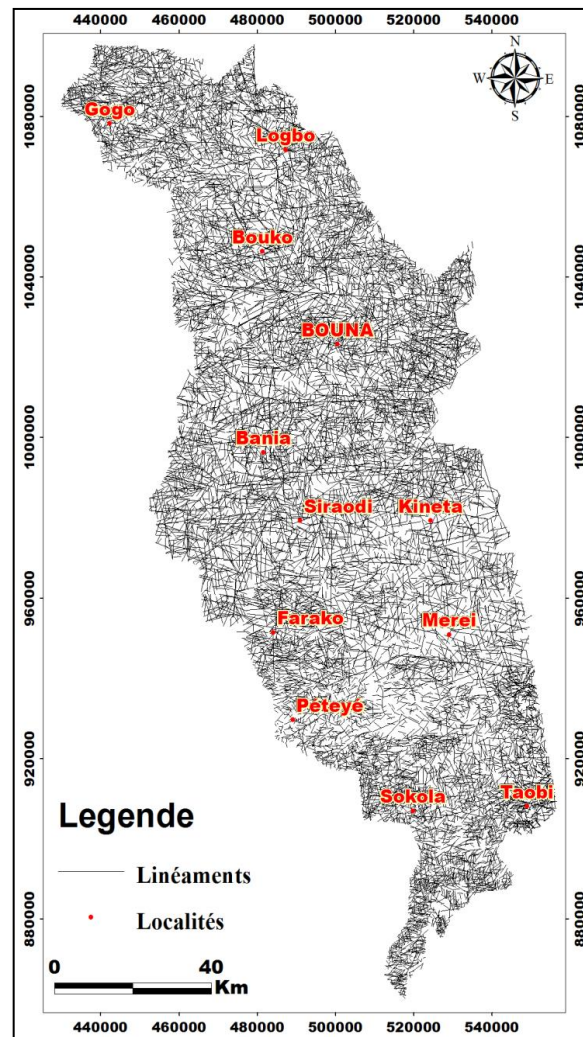


Figure 6. Lineaments map of the study area

➤ Statistical analysis of fracture networks

Statistical distribution

The lineaments network mapped counted have 12 596 lineaments. The lengths of lineament vary between 0.207 and 59.6 km and spread over two orders of magnitude, with an average and a standard deviation respectively of 3 and 2.47 km. The coefficient of variation Cv is equal to 82%

indicating a strong dispersion in the distribution of lineaments lengths. This analysis indicate that 84.96% of the lineaments have lengths lower than 7 km. There is thus a strong prevalence of small features (< 7 km) which represent about 90.16% of frequency. One in addition notes the existence of extreme values in the series lengths occupying 8% of the frequencies.

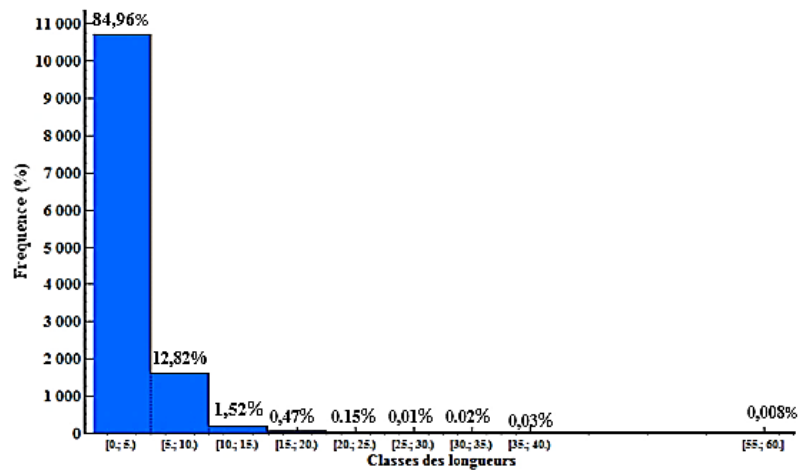


Figure 7. Histogram of Linear Length Distribution by Class

Rose diagram (figure a) shows the frequencies oscillate between 1 and 5%. The directions N00-10°, N10-20°, N70-80°, N80-90°, N90-100° and N170-180° emerge from the whole with frequencies ranging between 3 and 5%. On the cumulated lengths rose diagram, the same behavior is observed with frequen-

cies inferiors to 3%. The families N0-10°, N170-180° (4.5%), and N70-90° and N150°-160° (3%) emerge from the unit (figure 8=.

Generally, the spatial distribution of the features is homogeneous, indeed, no family of features does not exceed 10% in frequency.

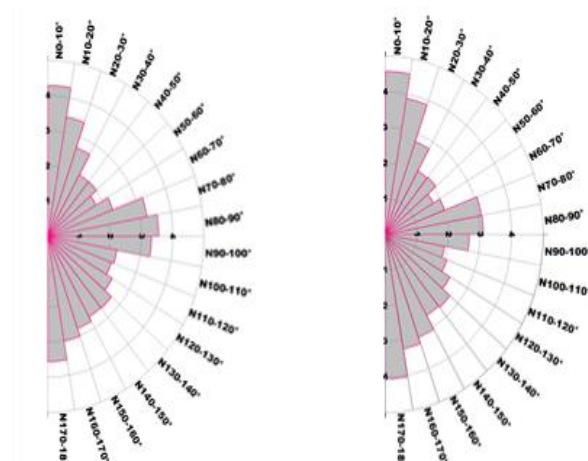


Figure 8. Directional distribution of the features a) Rose diagram expressed in number of lineaments: b) Rose diagram expressed in cumulative length of lineaments

With regard to spacings, 806 spacings were measured. These spacings vary between 1 and 10 370 m with an average spacing of 1 440 m and a standard deviation of 1569 m. the data of spacing also presenting a strong dispersion with a coefficient of variation $Cv = 109\%$. Indeed, nearly 56% of spacings are lower than 1 km.

➤ Validation of lineaments

Lineaments mapped was validated using former work available in the study area. On the rose diagram the repartition of fracture is homogeneous in the study area. Indeed, no family of fracture (directional) exceeds 10% in frequency. The results are the same that these of Youan Ta (2008). However, some families of fractures (NS, NW-SE), distinguish of others by their frequencies that oscillate between 3 and 5%.

The rest has very low frequencies and has considered minority, lineament of directional NE-SW are representative in Bondoukou area. The other directional (NS and EW) are minority.

The three directions NS (N00-10°; N170-180°); E-W (N70-80°; N80-90°); and NE-SW (N130-140°; N140-150°; N150-160°) meet as well at relatively significant frequencies on the rosette of the features of the zone of study (Figure 9)

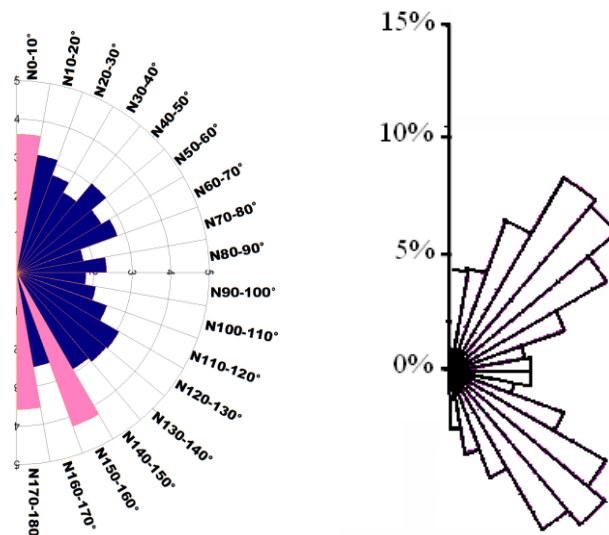


Figure 9. Rose diagrams; a) From this ; b) From Bondoukou area (Youan Ta, 2008).

Jofack-Sokeng, (2013) shows that the directional fracture s-so (N50-60°, N70-80° and N80-90°) and No- (N140-150°, and N150-160°) are the major directional in the square degree of Bondoukou. This author although has used an automatic method for lineament extraction and have confirmed the directions N70-80°; N80-90° (E-W) and N140-150°; N150-160° (NW-SE) such as majority.

Elsewhere, Coulibaly (2014) indicates in the Tanda, Koun-FAO and Transua areas that the major N90-100° (E-W) and N0-10° (NS) and secondarily fracturing are N70-80 (E-w-so) and N100-110 (ESE-WNW). These directions are the same that these obtained by Mangoua, (2013) in the Baya catchment (part of Comoe catchment, located at the south of the area).

In the same way, the concordance between the major fractures with the geological structures identified by Biémi (1992) and the hydrographic network confirm that the certain identified lineaments are most probably associated the fracturing (Lasm and Razack, 2001). Otherwise, all these observations contribute to the validity the mapped lineaments in the black Volta catchment in Côte d'Ivoire. Consequently, these lineaments can be assimilated to fractures.

➤ Statistical analysis of parameters of the fracturing

The lengths of fracture were analyzed using power law (figure 10). On the diagram we can distinguishes a linear portion on which it can be adjusted the power law ($\ell = 6.1$ km). His expression can be writing according equation 2:

$$N(\ell) = 3 \times 10^{13} \times \ell^{-2.937} \quad (2)$$

The coefficient of determination $R^2 = 0.9765$ can be regarded as significant. The adjustment following the power law remains valid for lengths of fracture higher than 6.1 km. The characteristic coefficient of the power law α is equal to 2.937, it translates a good interconnection between the long and the small fractures of the study area favorable for a good groundwater flow.

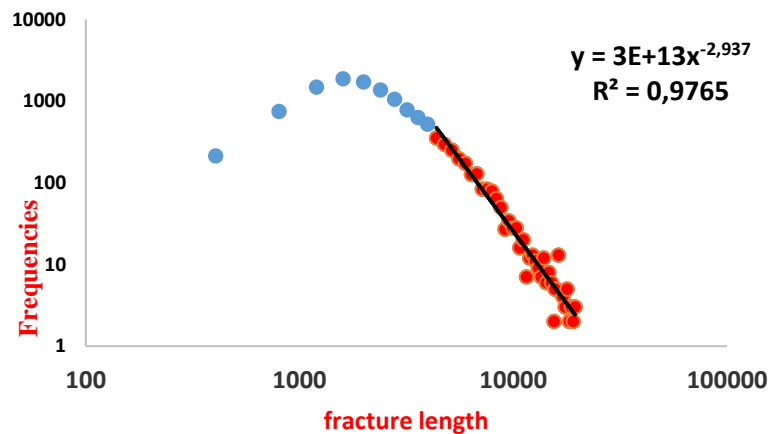


Figure 10. Log-log fracture length distribution. Adjustment according the Power law

Spacings were analyzed using main laws notably exponential negative, lognormal and gamma laws. Results of Khi-2 test at threshold of 10% were illustrated in table II.

This indicate that gamma law presents the best adjustment. Spacings of this area are distributed according gamma law.

Table 2. Results of Khi-2 test

distribution laws	Calculated Khi ²	Theoretical Khi ² (Threshold of 10%)	Degree of freedom
Exponential	13.46	15.09	5
Lognormale	29.75	16.81	6
Gamma	12.51	13.28	4

➤ Geostatistical analysis of the fracturing

The experimental variogram of global fracturing is presented at figure 11. This variogram presents a particular behavior characterized by three sills whose last seems incomplete. The practical ranges of two elementary variograms are respectively $a_1 = 34.5$ km and $a_2 = 60$ km.

This indicate that fracturing of this area is complex and is due to the existence of several structures at several scales. The fracturing is characterized by a multi-regionalization i.e. a multi-structuring. In other words, the deployment of the fracturing in space in not random but is structured.

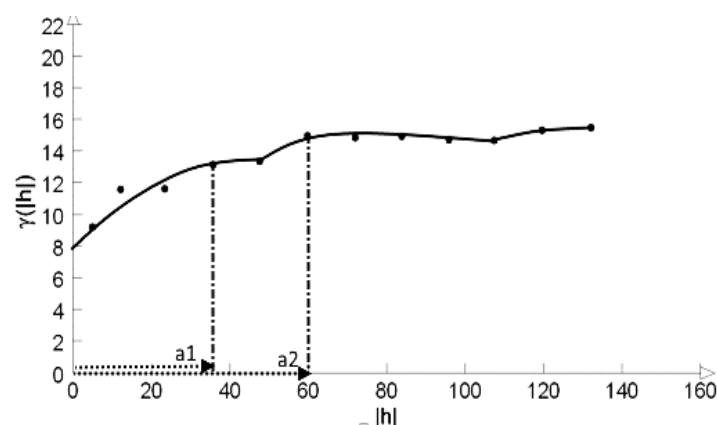


Figure 11. Variogram of gobal fracturing : ajustment to exponential model

The global variogram is the sum of two elementary variograms. The equations of the elementary variograms and the total global variogram of the fracturing are given by the expressions below (Eq. 3 to 5)

$$\gamma_1(h) = 7.14 + 11.82(1 - \exp(\frac{-3h}{34.5})) \quad (3)$$

$$\gamma_2(h) = 13.59(1 - \exp(\frac{-3h}{60})) \quad (4)$$

$$\gamma_{12}(h) = 7.14 + 11.82(1 - \exp(\frac{-3h}{34.5})) + 13.59(1 - \exp(\frac{-3h}{60})) \quad (5)$$

4. DISCUSSION

4.1. Structural mapping

The structural mapping is a first stage for any hydrogeological investigation in the crystalline basement. The techniques of pretreatment and treatment implemented led to the radiometric enhancement of the images that have permitted, the mapping of fracture of variable size. Indeed, with the ACPS approach, made it is possible to enhance the differences between the spectral properties of the images and thus facilitating the mapping of discontinuities (Jourda, 2005, Youan Ta, 2008). The index also has increased the contrast between the various geological entities (lithology) of the zone of study. The discontinuities images mapping was improved, thanks to the use of the directional filters (Sobel and gradient of Yésou et al., 1993). These methods were used successfully in many areas in Côte d'Ivoire: Man (Kouamé, 1999; Lasm, 2000), Korhogo (Jourda, 2005), Soubré (Yao, 2009) and Tanda (Coulibaly et al., 2014). Also the quality of OLI imagery of Landsat 8 used in a study contributed to the improvement of the informations contained on these images.

The extraction of the lineaments by the manual method gave convincing results. A significant number of lineaments was mapped. Indeed, the study area is characterized by a strong density of fracturing who is the results of various tectonic events that have affected this area (Youan Ta, 2008; Youan Ta et al. 2008).

4.2. Analysis of fracturing

Statistical analysis of fracturing has allowed to have a better knowledge of the fractures network of the studied area. The lengths of fractures are distributed according to a power law. The characteristic coefficient (α

= 2.92) of this law is in agreement with the literature data ranging between 1 and 3 (Bodin and Razack, 1996; Lasm, 2000; Youan Ta et al, 2008; Koudou et al, 2013). According to these authors, this value so close to 3 is characteristic of fractures network percolant in which the long and the small fractures control the connectivity.

However this law does not take in account the fractures length, lower than 5725 m. Indeed, this law is not valid for these fractures. For their characterization, Lasm (2000) suggests a sampling on a scale smaller than that that studied here. For many authors (Lasm, 2000; De Dreuzy 2000; Darcel, 2002), this law is an indicator of stage of development of the fractures networks in terms of maturity. The fractures in the crystalline rocks are distributed according to a power law (Lasm et al, 2014). For Bonnet *et al.* (2001), the not very mature networks at small development or low maturity are distributed according to the exponential law, whereas the more mature networks follow a power law. This power law can be used as an indicator of development stage for the fracture networks. The fracture networks identified here has reached a stage of advanced development. Similar results were obtained by various authors (Bodin and Razack, 1999; Lasm, 2000, De Dreuzy, 2000; Jourda, 2005; Baka, 2012; Koudou et al, 2013; Lasm et al., 2014). For these authors, all the natural fractures networks at the end of their development have their lengths of fractures distributed according to a power law. It is the case of the fracturing in crystalline and cristallophyllienne rocks of the Precambrian basement of Cote d'Ivoire (Lasm, 2000; Jourda, 2005; Baka, 2012; Koudou et al, 2013; De Lasme, 2013). The power law seems a model good to represent the distributions lengths of fractures.

Spacing is a significant geometrical parameter of the fracturing which conditions the size of the fractured blocks and suitable for inform about the behavior and/or the permeability of the system of fractures (Lasm, 2000). It controls also the implementation of the new fractures (Rives et al., 1992; Lasm et al. 2014). The studies of spacings carried out in rocks of nature and competences different in the last decades have permitted to underline the

interest of this parameter in fracturing (Lasm, 2000, Lasm et al., 2014).

In spite of these many studies, the law of distribution of this parameter remains very controversial in the literature (Rives et al., 1992; references). However Rives et al., (1992), showed starting from analogical models and digital simulations of fracture networks which the distribution of spacing evolves with the development of fractures and deformation. It start of the negative exponential distribution to the normal distribution which corresponds at the final stage of development while passing by gamma and lognormal distribution.

The spacing distribution according gamma law indicates a development of the fracturing in the Paléo-protérozoïque basement of catchment of Black Volta. Similar results were obtained by various authors (Huang and Angelier, 1989; Lasm, 2000; Youan Ta, 2008). On the other hand, Bodin and Razack, (1999) and Baka (2012) showed that fractures spacing can be adjusted by the power law. In the same way, Pascal et al., (1997) and Odonne et al. (2007) showed that the distribution of fractures spacing was lognormal. This various studies highlights well the variability of this law of distribution whose explanations can be found in the sampling approach, window sampling, measurements errors, the competence of the operator, etc.

The geostatistical analysis of the fracturing indicates that the density of fracturing behaves like a regionalized variable. The behavior of the variogram at small and long distance indicated the present existence of nugget effect that translates the irregularity of the studied variable. This phenomenon is usually met in the geostatistical analysis of fractured media (Lasm et al., 2004; Youan Ta et al., 2008). The nugget effect is interpreted like the reminiscence of structures inaccessible on a scale studied and represents the sum of uncertainties of measurements. Its difficult on a variogram to separate the effect of uncertainties of measurements and the the reminiscence of structures (Lasm, 2000).

The nugget effect on the variogram represent **60,4** % of total variance and is less significant than that met in other studies undertaken in Côte d'Ivoire: Lasm (2000) in Man-Danané area (27.56%),

Jourda (2005) in the area of Korhogo (36,46 %), Baka (2012) in the area of Oumé (31,88 %) and close to Youan ta et al., (2008) in Bondoukou (77,38%) in the same area.

Results obtained here showed that the fracturing of study area is well developed and seems complex. Indeed, this fracturing present a multi-regionalization characterized by many structuring at different scale. The total practical range that equal to 60 km is important. Similar results have obtained by Youan Ta (2008) and Youan Ta et al. (2008) in Bondoukou area located at the south of the study area, where the global variogram is constituted of five elementary variograms which the practical rage is equal to 56 km. Bondoukou and Black Volta areas are so close i.e. neighboring areas. These two areas have affected probably by the same tectonics events and have similar geological history.

These results come to confirm the conclusion according to which, the fracturing of this area is complex (Youan ta et al, 2008).

5. CONCLUSION

The techniques of digital processing (ACPS, bands ratio, coloured composition) and of filtering of the images (Sobel, Gaussian 3x3 and filters of Yésou et al., 1993) of the satellite images allowed to mapped 12 596 lineaments with lengths oscillate between 0.2 and 59.6 km. The directions NS (N00-10°, N170-180°), E-o (N70-90°) and No- (N130-160°) represent the dominant orientations of the zone of study.

The statistical analysis showed that the distribution of the fracturing is homogeneous. The lengths of fractures are distributed according to the power law. This law characterizes the lengths of fractures higher or equal to 5 725 m. Spacing was distributed according is of gamma law. The fracture networks of the Black Volta area reached a stage of advanced development according to the statistical analyses.

The spraying of fracturing in the Black Volta area has structured, indeed, fracturing behaves like a regionalized variable. Global variogram presents a double regionalization with two practical ranges ($a_1 = 34.5$ km and $a_2 = 60$ km). Fracturing of this area is developed and complex.

All these results permit a good knowledge of fracturing of the Black Volta catchment in Côte d'Ivoire. These results make it possible to undertake the groundwater modeling on this catchment.

REFERENCE

1. Adon G.C., Kouame K.F., Sorokoby V.M., Brouyere S., Affian K. (2014). Automatic extraction of lineaments using Landsat-7 ETM + satellite imagery in Precambrian basement zone (Haute Marahoué, Ivory Coast). *International Scientific Review of Geomatics*, vol 1, n° 1, pp.30-39.
2. Baka D. (2012). Geometry, hydrodynamism and modeling of fractured reservoirs in the Proterozoic basement of the Oumé region (west-central Côte d'Ivoire). Unique thesis. University Felix Houphouet Boigny of Abidjan, 390p.
3. Bessoles B. (1977). *Geology of Africa: The West African craton*. Memory. B.R.G.M., France, no. 88, 403 p.
4. Biemi J. (1992). Contribution to the geological, hydrogeological and remote sensing study of sub-Saharan basins of the Precambrian basement of West Africa Hydrostructural, hydrodynamic, hydrochemical and isotopic discontinuous aquifers of furrows and granitic areas of the Haute Marahoué (Côte d'Ivoire). Doctoral thesis. Nat. Sc., Abidjan University, 493 p.
5. Bonnet E., Bour O., Odling N.E., Davy P., Main I.G., Cowie P.A., Berkowitz B. (2001). Scaling of fracture systems in geological media. *Review of Geophysics*, Vol. 39, pp. 347-383.
6. Cefigre (1992). *Hydrogenology of the Afrique de l'Ouest. Synthèse des connaissances du socle cristallin cristallophyllien et sédimentaire ancien*. Collection Maîtrise de l'eau 2ème Ed. pp.147
7. Coulibaly. A. T., Lasm, Kouadio K. E, W.F. Kouassi, De Lasme O. Z, Baka D, Yao K. T., Savane I., and Biemi J. (2014). Contribution of Electrical Resistivity Method to the Location of Aquifers of Precambrian Basement in the Department of Tanda (North- Eastern Côte d'Ivoire), *Journal of Scientific Research & Reports*, 3 (5), pp. 723-741,
8. De Sève, and Desjardins, R. (1994). Contribution of radar data from ERS-1 in the apprehension of the organization of lineaments: the case of the Astoblème de Charlevoix, *Canadian Journal of Remote Sensing*, Vol. 20, No. 3, pp. 233-244.
9. De Dreuzy, J.R., Davy, P., Bour, O. (2000) Percolation threshold of 3D random ellipses with widely-scattered distributions of eccentricity and size. *Physical Review E*, 62, pp. 5948–5952.
10. Dewandel B., Lachassagne P., Wyns R., Marechal J.-C., Krishnamurthy N.S. (2006). A generalized 3-D geological and hydrogeological conceptual model of granite aquifers controlled by single or multiphase weathering. *Journal of Hydrology*, Vol.330, N°1-2, pp. 260-284.
11. Dibi B., Inza D., Goula B.T.A., Savane I. and Biemi J. (2004). Statistical analysis of the parameters influencing the productivity of water drilling in crystalline and crystallophyllian medium in the region of Aboisso (South-East of Côte d'Ivoire). *South Science & Technology*, Vol. 13, pp. 22-31
12. Hung L. Q., Batelaan O., De Smedt F. (2005). Lineament extraction and analysis, comparison of Landsat ETM and ASTER imagery. Case study: Suoimuoi tropical karst catchment, vietnam, *Remote Sensing for Environmental Monitoring, GIS Applications, and Geology V. spiel Brugge (Belgium)*, 59830T- 12p.
13. Jofack-Sokeng V.-C., Kouame K. F., Youan Ta M., Saley M. B., Kouame K. (2014). Automatic extraction of lineaments on satellite images by neural networks: contribution to the structural mapping of the Precambrian basement of the Bondoukou region (north-eastern Côte d'Ivoire), *International Scientific Review of Geomatics*, vol. 1, No. 1, pp. 4-17.
14. Jourda J. P. (2005). Methodology of application of remote sensing techniques and geographic information systems to the study of fissured aquifers of West Africa. Concept of space hydrotechnics: case of the test areas of Côte d'Ivoire. State Doctorate Thesis, University of Cocody, 430p.
15. J. Jourda, Saley M. B., Djagoua E. V., Kouame K., J., Biemi J., Razack M. (2006). Use of Landsat ETM + and GIS data for assessment of groundwater potential in cracked media Precambrian of the Korhogo region (Northern Côte d'Ivoire): multicriteria analysis and validation test approach. *Remote Sensing Review*, Vol. 5, No. 4, pp. 339-357.

16. Koita M. (2010). Characterization and modeling of the hydrodynamic functioning of a fractured aquifer in a basement area. Region of Dimbokro-Bongouanou (Central East of Côte d'Ivoire). Ph.D. thesis, University of Montpellier II, 220 p
17. Kouamé K. F. (1999). Hydrogeology of discontinuous aquifers in the semi-mountainous region of Man-Danané (western Côte d'Ivoire). Data input from satellite images and statistical and fractal methods to the development of a hydrogeological information system with spatial reference. Thesis 3rd cycle, University. Cocody Abidjan, (Ivory Coast), 194 p.
18. Kouamé K.F., Gioan P., Biemi J., Affian K. (1999). Method mapping discontinuities satellite images: Example of the semi-mountainous region in western Côte d'Ivoire. Remote sensing, Vol. 2, pp.1-18.
19. Koudou A., Assoman V. Adiaffi. B., Youan Ta M., Kouame K. F. Lasm T. (2014). Statistical and Geostatistical Analysis of Fracturing Extracted from ENVISAT ASAR Imaging in the Southeast Ivory Coast, Larhyss Journal, No. 20, pp. 147-166.
20. Lacombe J-P. (2008). Initiation au traitement d'images initiation au traitement d'images satellitaires, E.N.S.A.Toulouse, 92 p.
21. Lasm T., Youan Ta M., Jourda J. P., Kouame K. F. (2008). Fracture network analysis in basement area: case of the region of Bondoukou (north-is from Ivory Coast)
22. Mangoua J. (2013). Assessment of the potential and vulnerability of groundwater resources in cracked aquifers in the Baya watershed (eastern Côte d'Ivoire). Unique doctoral thesis, Nangui Abrogoua University, 171p.
23. Matheron G. (1970). The theory of regionalized variables and its applications. Notebook. C. Mr. M. Fontainebleau, Fasc. No. 5, 212 p. Massoud H., (1988). Modeling of the small fracking techniques geostatistics. Document B.R.G.M., pp. 155-197.
24. Odling N. E., Gillespie P., Bourgine B., Castaing C., Chilèsj.-P., Christensen N. P., Fillion E., Gender A., Olsen C., Thrane L., Trice R., Aarseth E., Walsh J.J., Watterson J. (1999). Variations in fracture system geometry and their implications for fluid flow in fractured hydrocarbon reservoirs, Petroleum Geoscience, n°5, 373–384.
25. Odonne F., Lezin C., Massonnat G., Escadeillas G. (2007). The relationship between joint aperture, spacing distribution, vertical dimension and carbonate stratification: An example from the Kimmeridgian limestones of Pointe-du-Chay (France). Journal of Structural Geology, Vol. 29, pp. 746-758
26. Otchoumou. K. F. Saley, M.B. Aké. G.E., Savané. I. (2012). Contribution of remote sensing and GIS in the identification of groundwater resources in the Daoukro region (East-Central Côte d'Ivoire), International Journal of Innovation and Applied Studies (ISSN), Vol. 1, no. 1, pp. 35-53.
27. Ouattara G., Koffi G.B. and Yao A.K. (2012). Contribution of Landsat 7 ETM + satellite imagery to lithostructural mapping in east-central Côte d'Ivoire (West Africa). International Journal of Innovation and Applied Studies, vol. 1, no. 1, pp. 61-75.
28. Pascal C., Angelier J., Cacas M.C., Hancock P.L. (1997). Distribution of joints: probabilistic modeling and case study near Cardiff (Wales, U.K.). Journal of Structural Geology, Vol. 19, N°10, pp. 1273-1284
29. Razack M., Lasm T. (2006). Geostatistical estimation of the transmissivity in a highly fractured metamorphic and crystalline aquifer (Man- Danané Region, Western Côte d'Ivoire). Journal of Hydrology, Vol.325, N°1-4, pp. 164-178
30. Rives T., Razack M., Petit J. P., Rawnley K. D. (1992). Joints spacing: analogue and numerical simulations. J. Struct. Geol., Vol. 14, n°. 8/9, pp.925-937.
31. Saley Mr. B. (2003). Spatially Reference Information System, discontinuous pseudo-images and thematic mapping of water resources in the semi-mountainous region of Man (West of France). Ivory Coast), PhD thesis, University of Cocody, 209 p
32. Savane I. (1997). Contribution to the geological and hydrogeological study of discontinuous aquifers of the crystalline basement of Odienné (North-West of Côte d'Ivoire). Contribution of remote sensing and a spatially referenced

- geographic information system. PhD thesis in Natural Sciences. University of Cocody (Ivory Coast), 332 p.
33. Scanvic J. Y. (1983). Use of remote sensing in the earth sciences. BRGM Edition Manuals and Methods, Vol. 7, 160 p
 34. Sorokoby, M.V., Saley, M.B., Kouamé, K.F., Djagoua, E.V. and Biemi, J. (2010). Using Landsat Images ETM + and SIRS for lineament and thematic mapping of Soubre-Meagui (south-west of Ivory Coast): contribution to the management of groundwater resources, Review Remote sensing, vol. 9, no. 3-4, pp. 209-223.
 35. Tagini B., (1971). Structural sketch of Ivory Coast. Geotectonic test, Memory. SODEMI, 302 p.
 36. Wyns R., Baltassat J. M., Lachassagne P., Legchenko A., Vairon J., Mathieu F. (2004).
 37. Wyns R., Gourry J.-C., Baltassat J.-M., Lebert F. (1999). Multiparameter characterization of subsurface horizons (0-100 m) in an altered basement context. PANGEA, 31/32, pp. 51-54.
 38. Yace I. (2002). Initiation to geology. The example of Côte d'Ivoire and West Africa. CEDA edition. Abidjan. 183 p.
 39. Yao K. T. (2009). Hydrodynamism in crystalline and crystallophyllic basement aquifers of south-west Côte d'Ivoire: the case of the department of Soubré. Contribution of remote sensing, Geomorphology and Hydrogeochemistry, PhD Thesis, University of Cocody, Abidjan, 252 p. Yésou H., Besnus Y., Rolet J. and Pion J. C. (1993). Comparison and evaluation SPOT ERS-1 Seasat Landsat data and combined data from structural geology studies. In 8th Congr. Ass. Quebec Remote Sensing 16th Symp. Sherbrooke (Canada) pp.521-526.
- Youan Ta M. (2008). Contribution of remote sensing and geographical information systems to the hydrogeological prospection of the Precambrian basement of West Africa: Case of the Bondoukou region North East of Côte d'Ivoire. Ph.D. thesis of Cocody-Abidjan University 236 p
- Youan Ta M., Lasme O., Baka D., Lasm T., Jourda J. P., Biemi J. (2015). Analysis of the hydrodynamic properties of the fissured aquifer of the Paleoproterozoic basement: aid for the supply of drinking water to the populations of the

Bondoukou region (north-eastern Côte d'Ivoire). International Journal of Innovation and Applied Studies, Vol. 13 no. 3, pp. 561-580.